DOWNHOLE HETEROGENEOUS HEAT TRANSFER CHARACTERISTICS AND ROCK STRESS DISTRIBUTIONS INDUCED BY LIQUID NITROGEN JET

by

Chengzheng CAI*, Bo WANG, Yinrong FENG, Yanan GAO, and Yugui YANG

State Key Laboratory for Geomechanics and Deep Underground Engineering, Carbon Neutrality Institute, China University of Mining and Technology, Xuzhou, China

Original scientific paper
https://doi.org/10.2298/TSCI2404429C

Liquid nitrogen jet is expected to provide a new idea for the breaking of deep dry hot rock due to its low temperature. In order to study the characteristics of heterogeneous temperature and stress fields during liquid nitrogen jet impingement, the downhole flow and stress characteristics induced by liquid nitrogen jet were studied by a thermal-hydraulic-mechanical coupling model. The results showed that under the same conditions, the potential core and the maximum velocity of liquid nitrogen jet were higher than water jet. The liquid nitrogen jet had a larger region of high turbulent kinetic energy, and the heat transfer efficiency with the bottom rock was obviously higher than water jet. Compared with the water jet, the liquid nitrogen jet formed a tensile stress zone in the bottom rock. The research was expected to provide a theoretical basis for the rock breaking mechanism of liquid nitrogen jet.

Key words: *liquid nitrogen, jet, drilling, flow field, stress field*

Introduction

Hot dry rock (HDR) geothermal resources mainly occur in high temperature hard granite and metamorphic rocks with the uniaxial compressive strength of more than 200 MPa [1]. Therefore, there are many problems in HDR well drilling, such as serious bit wear and low rock breaking efficiency [2]. The high pressure water jet has been played an important role in drilling [3]. At present, a series of new jet methods have been proposed, such as supercritical CO_2 jet, thermal jet and liquid nitrogen jet.

Liquid nitrogen jet could form a huge temperature gradient in rock [4]. Consequently, the efficient breaking of high temperature rock is realized by coupled effect of jet impingement and thermal stress. Huang *et al.* [5] found that the rock breaking induced by liquid nitrogen jet was mainly characterized by bulk fragmentation. Zhang *et al.* [6] indicated that thermal cracks were formed on the rock surface as the high temperature rock was cooled rapidly by liquid nitrogen jet. In complex flow and heat transfer fields, Yang *et al.* [7-9] achieved abundant innovative results about fractal power law and scaling-law fluids, which could provide a new perspective for understanding the flow characteristics of liquid nitrogen jets. In this work, the heterogeneous heat transfer characteristics and stress distribution induced by liquid nitrogen jet were discussed by comparing with the results of water jet.

* Corresponding author, e-mail: caicz@cumt.edu.cn

Numerical model

Problem description and geometric model

Liquid nitrogen jet impingement on rock is a complex multi-field coupling process involving transient flow field, conjugate heat transfer and solid deformation at the same time. In order to study the flow and stress fields in the downhole region during jet impingement, a geometric model was established as shown in fig. 1. The model consisted of two parts: solid domain and fluid domain. The fluid domain consisted of the inner region of the nozzle and the annulus region around the wellbore. The space between the nozzle outlet and the bottom of well was defined as the downhole region, and the space between the drill pipe and the surrounding rock is defined as the annulus. The solid domain was the rock around the wellbore. The model parameters were shown in tab. 1.

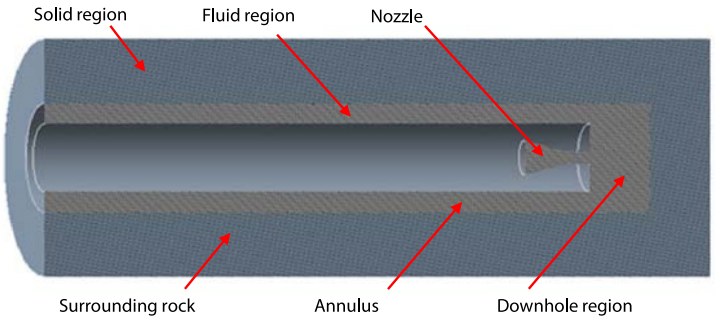

Figure 1. The geometric model for downhole flow and stress fields of liquid nitrogen jet

Table 1. Model parameters

Wellbore height	Wellbore diameter	Drilling diameter	Rock thickness	Model height	Standoff distance	Nozzle outlet diameter
300 mm	50.8 mm	31.8 mm	30 mm	330 mm	30 mm	6 mm

Mathematical model

The liquid nitrogen jet process involves heat transfer and fluid compressibility. In addition solving the mass conservation equation and momentum equation, the energy equation should also be solved [10, 11]:

$$\frac{\partial \rho_f}{\partial t} + \frac{\partial (\rho_f u_i)}{\partial x_i} = 0 \tag{1}$$

$$\frac{\partial \left(\rho_f u_i\right)}{\partial t} + \frac{\partial \left(\rho_f u_i u_j\right)}{\partial x_j} = -\frac{\partial p}{\partial x_i} + \frac{\partial}{\partial x_i}\left(\mu \frac{\partial u_i}{\partial x_j}\right) + S_i \tag{2}$$

$$\frac{\partial \left(\rho_f T_f\right)}{\partial t} + \frac{\partial \left(\rho_f u_i\right)}{\partial x_i} = S_T + \frac{\partial}{\partial x_i}\left(\frac{k_h}{c_p}\frac{\partial T_f}{\partial x_i}\right) \tag{3}$$

where t is the time, ρ_f – the density, u_i – the velocity component, x_i and x_j – the displacement components, μ – the viscosity, k_h – the fluid thermal conductivity, c_p – the specific heat of fluid, and S_i and S_T – the source terms of momentum conservation and energy conservation equations, respectively.

Due to the heat transfer effect of rock in the solid region, the heat conduction equation should be solved in the solid region:

$$k_s \nabla^2 T_s = c_s \rho_s \frac{\partial T_s}{\partial t} \tag{4}$$

The jet pressure and heat transfer during liquid nitrogen impingement would affect the internal stress field of the rock. It was necessary to calculate the physical equation, equilibrium equation and compatibility equation in the solid domain. The governing equations were given:

$$\varepsilon_{ij} = \frac{1}{2G}\left(\sigma_{ij} - \frac{\nu}{1+\nu}\sigma_{kk}\delta_{ij}\right) + \alpha \Delta T_s \delta_{ij}, \ \frac{\partial \sigma_{ij}}{\partial x_j} + F_i = 0, \ \varepsilon_{ij} = \frac{1}{2}\left(\frac{\partial u_i}{\partial x_j} + \frac{\partial u_j}{\partial x_i}\right) \tag{5}$$

where E is the elastic modulus, G – the shear modulus, υ – the rock Poisson's ratio, α – the rmal expansion coefficient, ε_{ij} – the rock strain, σ_{ij} – the rock stress, σ_{kk} – the sum of total stresses, δ_{ij} – the Kronecker symbol (its value is specified as 1 when $i = j$ and 0 when $i \neq j$), ΔT_s – the temperature gradient of the rock, F_i – the volume force in direction i, and u_i – the displacement in i direction.

Boundary conditions

As the fluid entered from the nozzle inlet, the jet impingement effect was formed by spraying into the wellbore under the nozzle, and then flowed out along the annulus of the wellbore. Therefore, the inlet of the nozzle was set as the pressure inlet boundary, the annular outlet of the wellbore was set as the pressure outlet boundary. The interface between the fluid and the solid part was set as the fluid-solid conjugate boundary. Conjugate heat transfer was used to calculate heat transfer at the fluid-solid interface. The k-ε model was used to calculate the turbulence flow. The simulation parameters were shown in tab. 2.

Table 2. Stimulation parameters

Parameter	Liquid nitrogen jet	Water jet	Rock
Inlet pressure [MPa]	45	45	–
Outlet pressure [MPa]	25	25	–
Initial fluid temperature [K]	110	298.15	–
Initial rock temperature [K]	423.15	423.15	–
Density [kgm^{-3}]	806.08	998.2	2300
Dynamic viscosity [Pa·s]	$1.6065 \cdot 10^{-4}$	$10.03 \cdot 10^{-4}$	–
Thermal conductivity [Wm^{-1}K^{-1}]	0.14581	0.6	2.5
Specific heat capacity [Jkg^{-1}K^{-1}]	2.0415	4.182	760
Yong's modulus [GPa]	–	–	30
Poisson's ratio	–	–	0.25

Results and analysis

Flow field

The velocity contours of liquid nitrogen jet and water jet were obtained, as shown in fig. 2. During the simulation, the inlet pressure, outlet pressure and jet time were 45 MPa, 25 MPa, and 10 seconds, respectively. At the outlet of nozzle, the velocity of the water jet was obviously lower than liquid nitrogen jet, and the velocity attenuation of the water jet was faster than liquid nitrogen jet. In addition, the high velocity region of the water jet was also smaller

than liquid nitrogen jet. For example, the velocity of the potential core region of the water jet was about 20 m/s lower than liquid nitrogen jet.

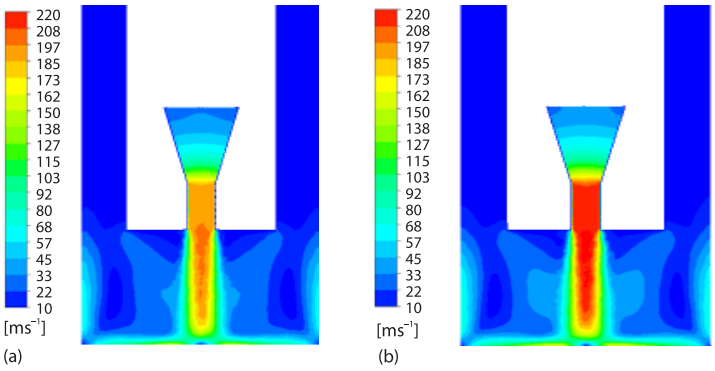

Figure 2. Velocity contours; (a) water jet and (b) liquid nitrogen

As shown in fig. 3, the high turbulent kinetic energy region was near the well bottom surface and the jet. Not only the turbulent kinetic energy of the liquid nitrogen jet was larger than that of the water jet, but also the liquid nitrogen jet had a larger high turbulent kinetic energy region. Thus, liquid nitrogen jet had stronger heat exchange capacity than water jet and was expected to produce greater thermal stress at the bottom.

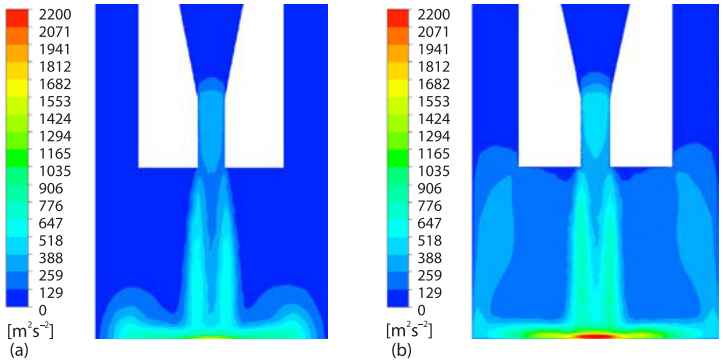

Figure 3. Turbulent kinetic energy; (a) water jet and (b) liquid nitrogen jet

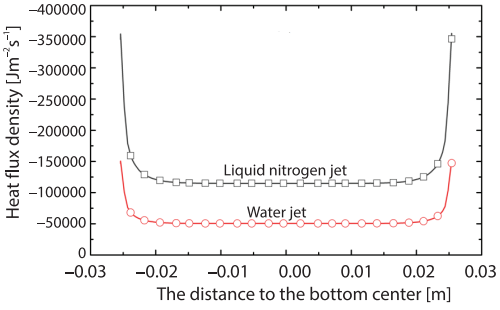

Figure 4. The heat flux density s in the bottom

Heat transfer characteristics

As shown in fig. 4, the heat flux density between fluid and rock was heterogeneous and the heat flux density in the bottom induced by liquid nitrogen jet was about 2.5 times higher than water jet. This indicated that the heat transfer efficiency of liquid nitrogen jet was much higher than water jet. In addition, the inhomogeneity of heat flux density induced by liquid nitrogen jet was obviously higher than that induced by water jet. In this case, the more heterogeneous stress fields would be created in the surrounding rock.

Stress field

The distributions of maximum principal stress at the depths of 2 mm and 10 mm from the bottom were analyzed. The jetting time was set as 1 seconds, 10 seconds, 30 seconds, and 120 seconds. As shown in fig. 5, the maximum principal stress in the center of the rock was negative, which was the largest negative value in the same horizontal plane. Away from the center of the bottom, the stress value was positive, indicating that the tensile stress zone began to appear around the jet impact location. At the depth of 2 mm, the central region of the rock was subjected to compressive stress while both ends were subjected to tensile stress due to liquid nitrogen impingement at 1 seonds. As the time increased to 10 seconds, the whole area of this depth was transformed into tensile stress. However, for the water jet, the central region at the depth of 2 mm was always subjected to compressive stress. This indicate that liquid nitrogen was helpful to form a tensile failure zone between the center of jet and the surrounding area. At the depth of 10 mm, the rock was always subjected to compressive stress due to both water jet and liquid nitrogen jet with the time increasing from 1-10 seconds. During this process, the compressive stress caused by water jet impingement kept constant, however, caused by liquid nitrogen jet decreased as time passed by.

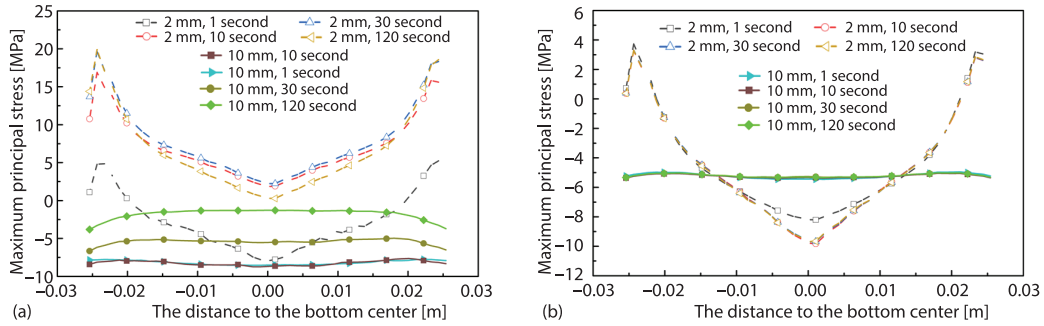

Figure 5. Bottom maximum principal stress distributions along radial direction; (a) induced by water jet and (b) indued by liquid nitrogen jet

Conclusion

In this work, the heat transfer characteristics and rock stress distributions in downhole region induced by liquid nitrogen jet were researched. The results showed that under the same conditions, the unstable turbulence region of the liquid nitrogen jet was stronger than that of the water jet. The heat flux generated at the bottom by liquid nitrogen jet was about 2.5 times higher than that of the water jet. Thus, the liquid nitrogen jet could produce significant tensile stress in the bottom rock, reduce the rock holding effect and improve the rock breaking efficiency.

Nomenclature

c_p – specific heat capacity, [Jkg^{-1}K^{-1}]
E – elastic modulus, [MPa]
G – shear modulus, [MPa]
k – thermal conductivity, [Wm^{-1}K^{-1}]
q_w – heat flux, [Wm^{-2}]
u – velocity, [ms^{-1}]

Greek symbols

α – thermal expansion coefficient, [Wm^{-1}K^{-1}]
δ_{ij} – Kronecker symbol
ε_{ij} – rock strain
μ – viscosity, [Pas]
ρ – density, [kgm^{-3}]
σ_{ij} – rock stress, [Mpa]
σ_{kk} – sum of total stresses, [MPa]
υ – Poisson's ratio

Acknowledgment

This research was funded by the National Key R&D Program of China (Grant No. 2022YFE0129100), Fundamental Research Funds for the Central Universities (Grant No. 2024KYJD100) and Project funded by China Postdoctoral Science Foundation (Grant No. 2019M650120).

References

[1] Liu, W. L., *et al.*, Drilling Difficulties and Solutions for Hot Dry Rock Geothermal Development, *China Petroleum Machinery*, *43* (2015), 43, pp. 11-5
[2] Li G., *et al*., Status and Challenges of Hot Dry Rock Geothermal Resource Exploitation, *Petroleum Science Bulletin*, *7* (2022), 03, pp. 343-364
[3] Li, G., *et al*., Research and Applications of Novel Jet Techniques in Well Drilling, Completion and Fracturing, *Science Foundation in China*, *22* (2014), 2, pp. 68-80
[4] Cai, C., *et al*., Numerical Simulation of the Flow Field Structure of Liquid Nitrogen Jet, *Thermal Science*, *23* (2019), 3A, pp. 1337-1343
[5] Huang, Z., *et al*., Mechanism of Drilling Rate Improvement Using High-Pressure Liquid Nitrogen Jet, *Petroleum Exploration and Development*, *46* (2019), 4, pp. 768-775
[6] Zhang, S., *et a*l., Experimental Study of Thermal-Crack Characteristics on Hot Dry Rock Impacted by Liquid Nitrogen Jet, *Geothermics*, *76* (2018), Nov., pp. 253-260
[7] Yang, X. J., An Insight on the Fractal Power Law Flow: From a Hausdorff Vector Calculus Perspective, *Fractals*, *30* (2022), 3, 2250054
[8] Yang, X. J., *et al*., On the Theory of the Fractal Scaling-Law Elasticity, *Meccanica*, *57* (2022), July, pp. 943-955
[9] Yang, X. J., *et al.*, A New Insight to the Scaling-Law Fluid Associated with the Mandelbrot Scaling Law, *Thermal Science*, *25* (2021), 6, pp. 4561-4568
[10] Batchelor, G. K., *An Introduction Fluid Dynamics*, Cambridge University Press, Cambridge, UK, 2000
[11] Zhang, S., *et al.*, Numerical Analysis of Transient Conjugate Heat Transfer and Thermal Stress Distribution in Geothermal Drilling with High-Pressure Liquid Nitrogen Jet, *Applied Thermal Engineering*, *129* (2018), Jan., pp. 1348-1357

Paper submitted: March 15, 2024
Paper revised: March 28, 2024
Paper accepted: May 16, 2024